Image-potential states at surfaces and in tunnel junctions

Cz. Oleksy, Abdellatif Akjouj, Leonard Dobrzynski

Image-potential states at surfaces and in tunnel junctions

Cz. Oleksy
Institute of Theoretical Physics, University of Wroclaw, ulica Cybulskiego 36, PL-50-205 Wroclaw, Poland

A. Akjouj and L. Dobrzynski
Equipe Internationale de Dynamique des Interfaces, Laboratoire de Dynamique des Cristaux Moléculaires, Unité de Formation et de Recherche en Physique, Université de Lille I, 59655 Villeneuve d'Ascq CEDEX, France
(Received 26 January 1990)

We report a theoretical study of image-potential states at a (001) surface of Ag, done with the help of a simple tight-binding model having an electronic band of finite width. The wave function associated with these states is calculated at the center of the two-dimensional (2D) Brillouin zone. The energy dispersion of these states is studied along symmetry directions of this 2D Brillouin zone and the deviation of this dispersion from its usual parabolic form is discussed. Inside a tunnel junction Ag(001)/vacuum/Ag(001) the energies of these image-potential states were shown to depend on the width of the vacuum slab. Finally, we report how the energies of these image-potential states vary when a voltage is applied to this junction.

I. INTRODUCTION

The observation of image-potential states with inverse photoemission and two-photon photoemission has stimulated interest in the fundamental character of these states. References to most of the past experimental and theoretical papers devoted to these image-potential states can be found in recent papers.[1-7]

The paper is mostly devoted to the study of these image-potential states within a Ag-vacuum-Ag tunnel junction. The energies of these electronic surface localized states are shown to depend on the width of the vacuum slab and are also a function of the magnitude of the voltage applied to this junction.

But before going to the case of the tunnel junction, we present first the principal characteristics of the image-potential surface states, within an original approach.

II. IMAGE POTENTIAL SURFACE STATES

In a previous paper[8] we studied surface states of a metal which was described by a tight-binding model. The influence of work function on the surface states was taken into account assuming a square potential barrier outside the surface. In such simple models we were able to study the properties (dispersion) of crystal-induced surface states. Here we study the image-potential surface states of a metal within a tight-binding aproximation. It is assumed that outside the metal surface there is an image potential of the following form:

$$\phi(z)=\begin{cases} E_b+cz & \text{for } 0<z<z_{\rm im}\ , \\ \phi_0-\dfrac{3.57}{z-z_0} & \text{for } z_{\rm im}<z<L\ , \\ \phi_0 & \text{for } z>L\ , \end{cases} \tag{1}$$

where E_b is the minimal energy of an electron in the crystal, ϕ_0 is the work function (Fermi energy $E_F=0$), and L denotes the range of the Coulombic part of the potential. The constant c is determined from continuity condition at $z=z_{\rm im}$ and the parameters $z_{\rm im}$ and z_0 are usually chosen to fit experimental data.[2,3] The units of energy and distance are electron volts and angstroms, respectively.

The surface states of the model are examined here using the interface response theory of a composite system.[8,9] In order to find the response function of the system the potential (1) is replaced by a steplike one for $0<z<L$. The latter is constructed by introducing N planar interfaces which are parallel to the metal surface and equally distant one from each other. Hence there are $N-1$ vacuum slabs between $z=0$ and $z=L$ with the same width. The height of the rectangular barrier in each slab is determined by the value of the image potential at the position of the left interface.

In this approximation the system consists of semi-infinite metal ($z<0$), semi-infinite vacuum ($z>L$), and $N-1$ vacuum slabs between them. Because the response functions for all mentioned subsystems were already calculated[8] it is easy to calculate the response function of the system but the details are omitted here.

The method is applied to study the properties of surface states of Ag(100). We have chosen $z_{\rm im}=1.1$ Å and $z_0=-0.6$ Å which provides a good agreement of the calculated binding energy $\varepsilon_n=E_v-E_n$ of these surface states (see Table I) with experimental data for $k_\parallel=0$:[5] $\varepsilon_1=0.52\pm0.02$ eV, $\varepsilon_2=0.16\pm0.02$ eV. If $E_F=0$ here, then $E_v=\phi_0$. The number of localized surface states depends, in this approach, on the range of the Coulombic potential, L (see Fig. 1). The energies ε_n in Table I were calculated for $L=1400$ Å and we have not listed the states whose energies were still L dependent. The hydrogeniclike image states form the series with binding ener-

TABLE I. The calculated binding energies ε_n for $k_\parallel=0$ of localized image-potential states for Ag(100) and their difference with the value $\tilde{\varepsilon}_n$ given by Eq. (2).

		$\frac{\varepsilon_n-\tilde{\varepsilon}_n}{\varepsilon_n}$ (%)	
		$a=0.268$	$a=0.256$
n	ε_n (eV)	$b=0$	$b=0.016$ eV
1	0.5287	0	0
2	0.1639	0.84	0
3	0.0787	1.09	0.07
4	0.0461	1.21	0.12
5	0.0300	2.00	0.57

gies well described by the formula

$$\tilde{\varepsilon}_n=\frac{0.85-b}{(n+a)^2}\ . \tag{2}$$

Putting $b=0$ into (2) one gets the commonly used expression since the work of Echenique and Pendry.[10] The parameter a is called a quantum defect. The comparison between the results calculated from (2) for $b=0$ and those obtained by the present theory are presented in column 3 of Table I. The last column shows that fitting with $b\neq 0$ leads to differences lower by 1 order. The crystal-induced surface state was found at energy $E_0=-3.724$ eV below the Fermi level.

Applying the method for calculating eignevectors of the composite system[11] we have obtained the wave functions of the surface states. The crystal-induced state [Fig. 2(a)] shows that the electron with energy E_0 is confined near the surface inside the metal but in the image-potential surface states E_1, E_2, and E_3 [Figs. 2(b)–2(d)] the electron is localized outside the metal.

The three-dimensional model presented above allows us to study the dispersion of surface states $E_n(k_\parallel)$ within the two-dimensional Brillouin zone of the square lattice. The results presented in Fig. 3 show that the dispersion of the crystal-induced state is similar to the dispersion of the top of bulk band whereas the dispersion of the image-potential surface states resembles the free-electron parabolic dependence of $k_\parallel$. However, a detailed examination yields the difference between the dispersion of image-potential states and the dispersion of free electrons (see Fig. 4) but this difference is below the experimental accuracy.[5] The dispersion of the crystal-induced state also exhibits deviations from cosine-type dependence up to ± 0.1 eV.

Similar calculations were performed for the metal in the free-electron approximation with the potential (1). The agreement with the experimental data was found for

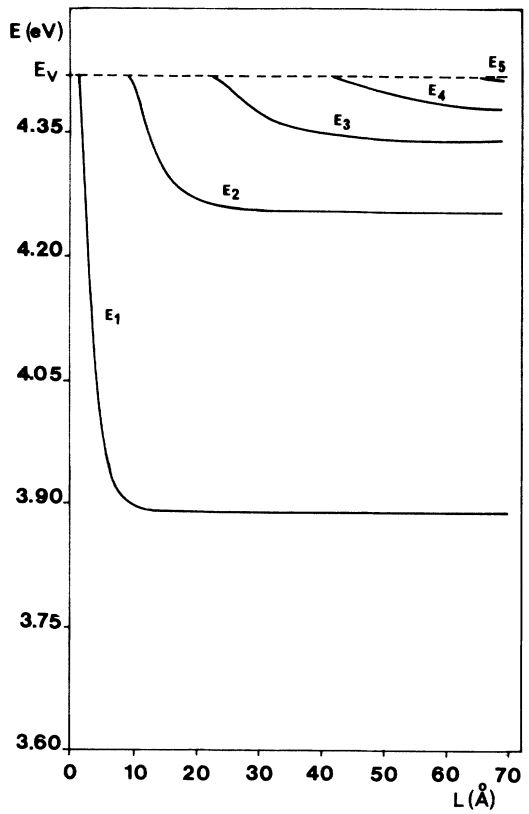

FIG. 1. Dependence of image-potential surface states energies $E_1, E_2, \ldots$, on the range L of the Coulombic part of the potential. $E_v=4.42$ eV denotes the vacuum level with respect to the Fermi level $E_F=0$.

$z_0=0.47$ Å and the dispersion of all surface states including the crystal-induced one is like the free-electron dispersion.

Finally we want to emphasize that taking into account the dispersion of the bulk band leads to small deviations from the parabolic dependence of the energy of image-potential surface states on the wave vector parallel to the metal surface. With the actual experimental accuracy these deviations from parabolic dependence were not observed.[5,6]

III. SURFACE STATES OF THE TUNNEL JUNCTION

It was shown[12–14] that the image potential plays an important role in the interpretations of vacuum tunneling experiments. Here we discuss properties of surface states of a system which consists of two similar metals separated by a thin vacuum slab of width L. The metal is described by a tight-binding model and in the vacuum there is the following image potential:

$$\phi(z)=\begin{cases} E_{b1}+c_1 z & \text{for } 0<z<z_{\rm im}\ , \\ \phi_0-7.14\left[\dfrac{1}{2(z-z_0)}+\displaystyle\sum_{n=1}^{\infty}\left[\dfrac{n(L-2z_0)}{[n(L-2z_0)]^2-(z-z_0)^2}-\dfrac{1}{n(L-2z_0)}\right]\right] & \text{for } z_{\rm im}<z<L-z_{\rm im}\ , \\ E_{b2}+c_2 z & \text{for } L-z_{\rm im}<z<L\ . \end{cases} \tag{3}$$

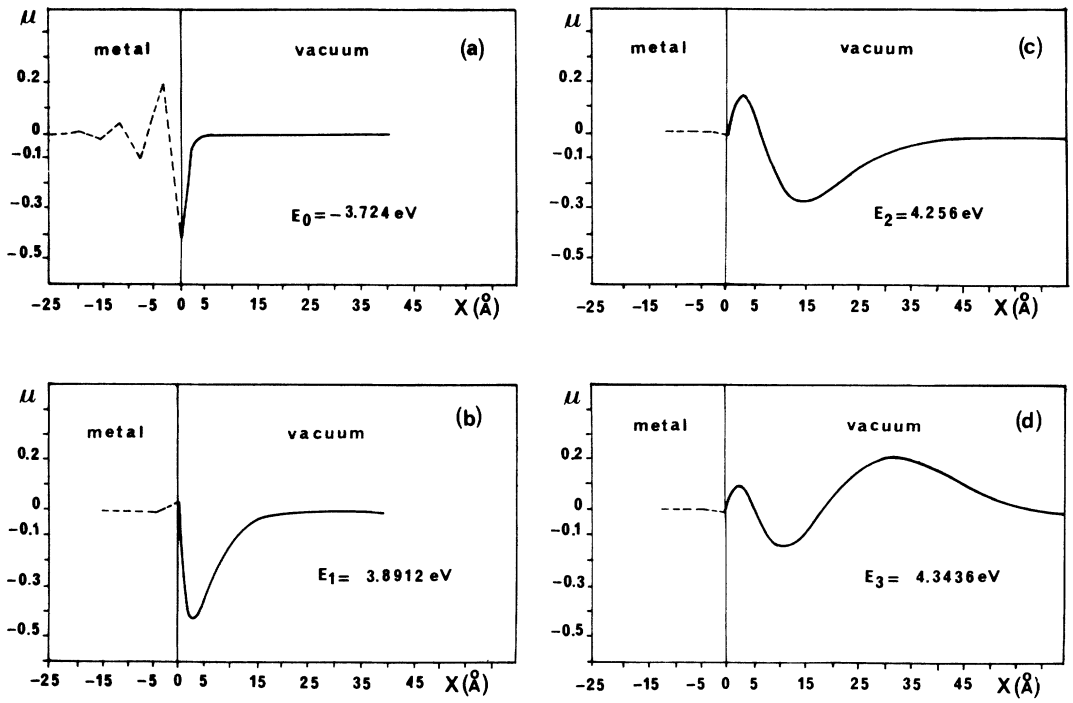

FIG. 2. The wave functions of the surface localized states.

E_{b1}, and E_{b2} are, respectively, the minima energies of electrons in the two metals. c_1 and c_2 are determined from continuity conditions at $z = z_{\text{im}}$ and $z = L - z_{\text{im}}$, respectively.

It is worth noting that the potential (3) reduces the height and the width of the rectangular barrier characterized by the work function ϕ_0.[15]

Fitting the potential (3) by a steplike potential, in a similar way as above, we can again calculate the localized states using the interface response theory.[8,9] The method is applied to the Ag-vacuum-Ag junction with the same parameters z_0, z_{im}, and ϕ_0 as in the preceding section.

For very small distances between the metal surfaces, $L \cong 6$ Å, there are only two localized states (crystal-induced states) with an energy separation of 0.002 eV. With increasing the distance L new image-potential states

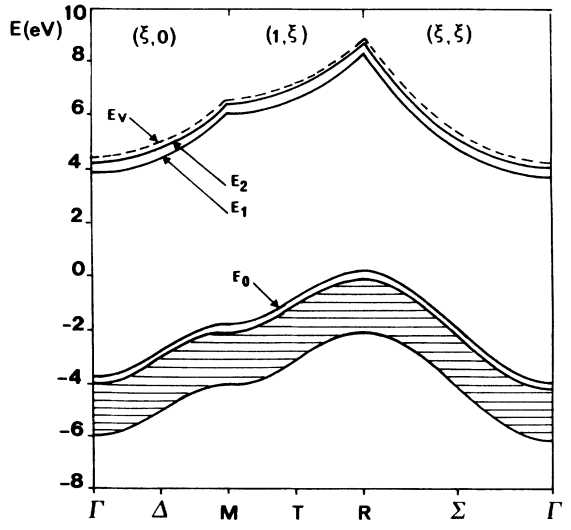

FIG. 3. Dispersion of surface localized states of Ag. The dashed area represents the bulk band and the dashed line the dispersion of free electrons with energy E_v at $k_{\parallel} = 0$. $\xi = k_i / k_{\max}$, $k_{\max} = \pi / a_0$, where a_0 is the lattice constant.

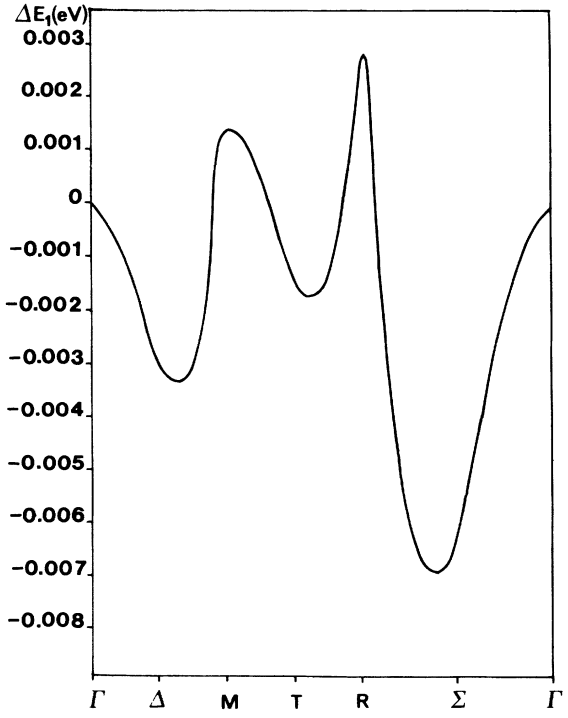

FIG. 4. The deviation ΔE_1 (eV) from free-electron dispersion of the first image-potential state

$$\Delta E_1 = E_1(0) + \hbar^2 k_{\parallel}^2 / 2m - E_1(\mathbf{k}_{\parallel}) .$$

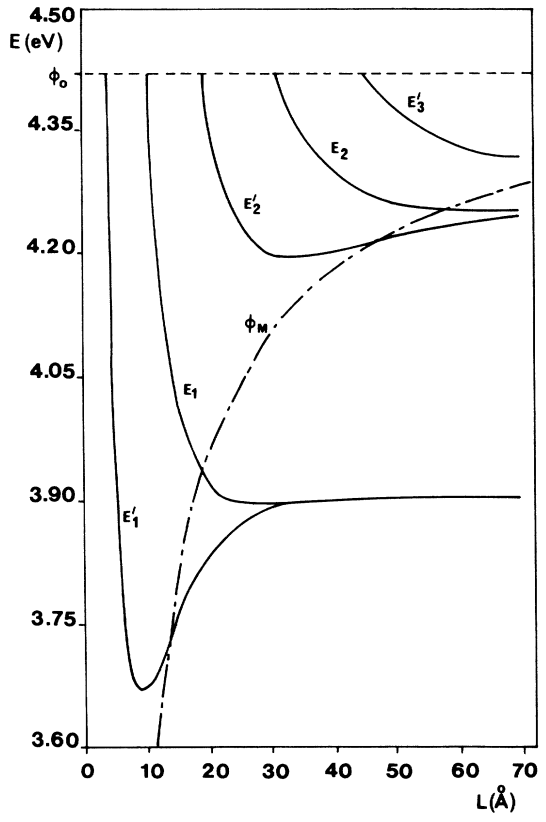

FIG. 5. The energies of localized surface states of the vacuum-Ag tunnel junction as a function of the distance L between metal surfaces. The dot-dashed line ϕ_m represents the maximum value of image potential, whereas ϕ_0 is the work function in the case of a rectangular barrier.

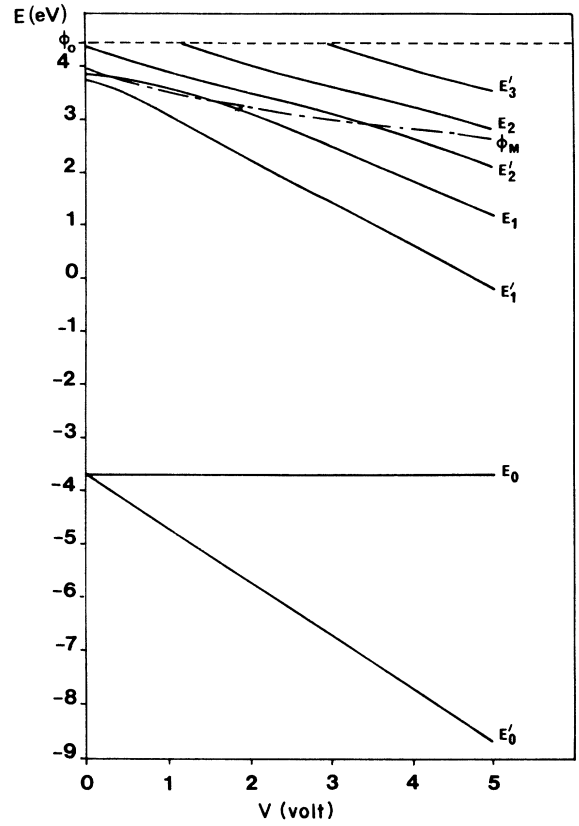

FIG. 6. Dependence of the energies of surface states of a tunnel junction Ag(001)/vacuum/Ag(001) on the voltage V for $k_{\parallel}=0$ and $L=20$ Å.

appear, E'_1 and E_1 (see Fig. 5), which for $L>35$ Å can be considered as one twofold degenerated state. A further increase of L leads to an appearance of new states, E'_2 and E_2, which are also degenerated for $L>80$ Å. A comparison between Figs. 1 and 5 shows that the levels of the degenerated states are nearly the same as the levels of the corresponding states in Fig. 1. This means that for each quantum number n of the surface states there exists a characteristic distance L_n. If the distance between the two metals is greater than L_n the surface states of the tunnel junction E'_n and E_n become similar to the states of the free surface.

Another interesting problem we want to discuss is the tunnel junction with an applied voltage V. The potential can be written as a sum of the image potential (3) and of the external field potential

$$\phi_{ex}=-V\frac{z}{L} . \tag{4}$$

It is assumed that the Fermi level of the positively biased electrode moves down linearly with applied voltage V.

The dependence of surface-state energies on voltage V for the distance between electrodes $L=20$ Å is presented in Fig. 6. The behavior of the crystal-induced states E_0 and E'_0 is different from the behavior of the image-potential states, whose energies vary nonlinearly with V. Moreover when the voltage increases one observes the appearance of new image-potential states.

IV. DISCUSSION

Using a simple tight-binding description of the (001) surface of Ag matched to the image Coulombic potential given by Eq. (1), we obtained the properties[1-7] of image-potential surface states: their energy dispersions (Fig. 3) and departures from parabolicity (Fig. 4) and their wave-function localization (Fig. 2). This model also provides crystal-induced surface state whose energy lies just above the bulk band of Ag (see Fig. 2).

Then we studied how the energies of these states vary in a Ag(001)/vacuum/Ag(001) tunnel junction. When the distance L between the two electrodes diminishes the wave functions of the image-potential states overlap, starting from the highest in energy image-potential states. This overlap produces first a shift in the energies of these states (Fig. 5). Then for a given value of L, each image-

potential state disappears. For $L \cong 6$ Å, only the two crystal-induced states remain. Finally, in Fig. 6, we show, for $k_{\parallel}=0$ and $L=20$ Å, the nonlinear value in applied voltage variation of the image-potential state energies.

ACKNOWLEDGMENTS

The Laboratoire de Dynamique des Cristaux Moléculaires is "unité associée au Centre National de la Recherche Scientifique No. 801."

[1]C. T. Chen and N. V. Smith, Phys. Rev. B **35**, 5407 (1987); **40**, 7487 (1989).

[2]N. V. Smith, C. T. Chen, and M. Weinert, Phys. Rev. B **40**, 7565 (1989).

[3]M. Steslicka, M. Zagorski, and L. Jurczyszyn, Surf. Sci. **200**, 209 (1989).

[4]Z. Lenac, M. Šunjić, H. Conrad, and M. E. Kordesch, Phys. Rev. B **36**, 9500 (1987).

[5]K. Giesen, F. Hage, F. J. Himpsel, H. J. Riess, W. Steinmann, and N. V. Smith, Phys. Rev. B **35**, 971 (1987); **35**, 975 (1987).

[6]A. Goldman, V. Dose, and G. Borstel, Phys. Rev. B **32**, 1971 (1985).

[7]R. O. Jones, P. J. Jennings, and O. Jepsen, Phys. Rev. B **29**, 6474 (1984).

[8]A. Akjouj, L. Dobrzynski, and Cz. Oleksy, Surf. Sci. **213**, 630 (1989).

[9]L. Dobrzynski, Surf. Sci. Rep. **6**, 119 (1986).

[10]P. M. Echenique and J. B. Pendry, J. Phys. C **11**, 2065 (1978).

[11]L. Dobrzynski and H. Puszkarski, J. Phys. Condens. Matter **1**, 1239 (1989).

[12]G. Binning, N. Garcia, H. Rohrer, J. M. Soler, and F. Flores, Phys. Rev. B **30**, 4816 (1984).

[13]G. Binning, K. H. Frank, H. Fuchs, N. Garcia, B. Reihl, H. Rohrer, F. Salvan, and A. R. Williams, Phys. Rev. Lett. **55**, 991 (1985).

[14]R. Garcia, J. J. Saenz, J. M. Soler, and N. Garcia, Surf. Sci. **181**, 69 (1987).

[15]J. G. Simmons, in *Tunneling Phenomena in Solids,* edited by E. Burstein and S. Lundqvist (Plenum, New York, 1969).